

## Research Paper

### Effects of Hole Perpendicularity Error on Load Distribution in Single-Lap Double-Bolt Composite Joints

Rupeng LI<sup>1)</sup>, Ruiheng XIAO<sup>1)</sup>, Ende GE<sup>1)</sup>, Hang GAO<sup>2)</sup>,  
Yongjie BAO<sup>2)</sup>, Xueshu LIU<sup>3)</sup>

<sup>1)</sup> *Shanghai Aircraft Manufacturing Co. Ltd.*  
Shanghai 200120, P.R. China

<sup>2)</sup> *School of Mechanical Engineering*  
*Dalian University of Technology*  
Dalian 116024, P.R. China

<sup>3)</sup> *School of Automotive Engineering*  
*Dalian University of Technology*  
Dalian 116024, P.R. China  
e-mail: liuxs@dlut.edu.cn

Although automated machines are widely used in composite structure manufacturing, manually drilled holes are usually necessary due to spatial constraints and holes with perpendicularity errors are occasionally generated as a result. Considering the anisotropic properties of composite material, the influences of hole perpendicularity error on mechanical performances of composite joints are different from those of isotropic material. In this study, the effects of hole perpendicularity error on load distribution in single-lap double-bolt composite joints are discussed. A finite element model is first developed and verified both by analytical and experimental results. Parametric studies are then carried out taking into consideration bolt torque and hole perpendicularity error, represented by hole tilting direction and tilting angle. It is found that the hole tilting direction significantly affects on load distribution in composite joints. Although the loads taken by bolts are not significantly affected, it may make one composite plate take more than 60% of total loads. In addition, the influences of tilting angle on load distribution can be ignored in most cases, and as for the bolt torque, it is to enhance the influence of hole tilting direction.

**Key words:** bolted joints; perpendicularity error; tilting direction; load distribution.

#### 1. INTRODUCTION

Due to the excellent features such as being easy to assemble and disassemble, high reliability and load-carrying capacity, bolted joints are widely used to fasten composite components together. Their joining, however, remains problematic

because of the brittle and anisotropic nature of many composite materials. The joints have to be carefully designed so as to limit the stresses around the bolt holes. It has been found that the load distribution in bolted joints significantly affect the stress concentration around the hole. For this reason, an accurate analysis of load distribution in multi-bolt composite joints is a critical step in designing reliable composite structures.

Load distribution could be influenced by many factors, including bolt-hole clearance [1–4], joint thickness [5], bolt torque [6, 7], and bolt profile [8]. Many researchers have focused on this issue for several decades. For example, McCarthy and Gray reported an analytical model to predict load distribution in highly-torqued multi-bolt composite joints [6]. In the present model, the effect of varying bolt-torque and bolt-hole clearance on load distribution in a three-bolt, single-lap joint is investigated. LIU *et al.* [5] proposed a model to predict the load distribution of multi-bolt single-lap thick laminate joints. It was found that bolt diameters, row distances and stiffness ratio greatly impacted the load distribution. SHAROS *et al.* [9] advanced the spring-based method to account for the loading rate effects and bearing damage. With their model, an accurate prediction of load displacement response of composite joints could be obtained within seconds. LECOMTE *et al.* [10] proposed an analytical model to evaluate the load distribution in an aluminum-composite double-lap joint, in the presence of clearance and hole-location errors. The nonlinear behavior of the bolt implied by bearing degradation was also taken into consideration in their model. TAHERI-BEHROOZ *et al.* [11] presented an analytical approach to determine load distribution in single-column multi-bolt composite joints and it was found that the load-displacement curve of the joint revealed between 3.66% and 3.97% more displacement at constant force in comparison to the linear case of three, and five bolted joints. Load distribution in hybrid joint attracts researchers attention, too [12, 13].

Although, as mentioned above, many factors have been investigated for their effects on the load distribution in multi-bolt composite joints, hole perpendicularity error has attracted little attention so far. When bolt holes are drilled, usually from one side of the assembly to the other, not all of them are machined as perfectly as expected all the time during assembly, and hole perpendicularity error sometimes occurs. When a bolt is fastened in such a tilting hole, assembly stresses around the hole are no longer even and residual forces generate in the composite joint as a result (Fig. 1), which consequently affects the load distribution in multi-bolt composite joints.

It is obvious that the residual forces depend on hole perpendicularity error and the bolt torque as well. The purpose of this study is to investigate the influences of the mentioned parameters on the load distribution in multi-bolt composite joints.

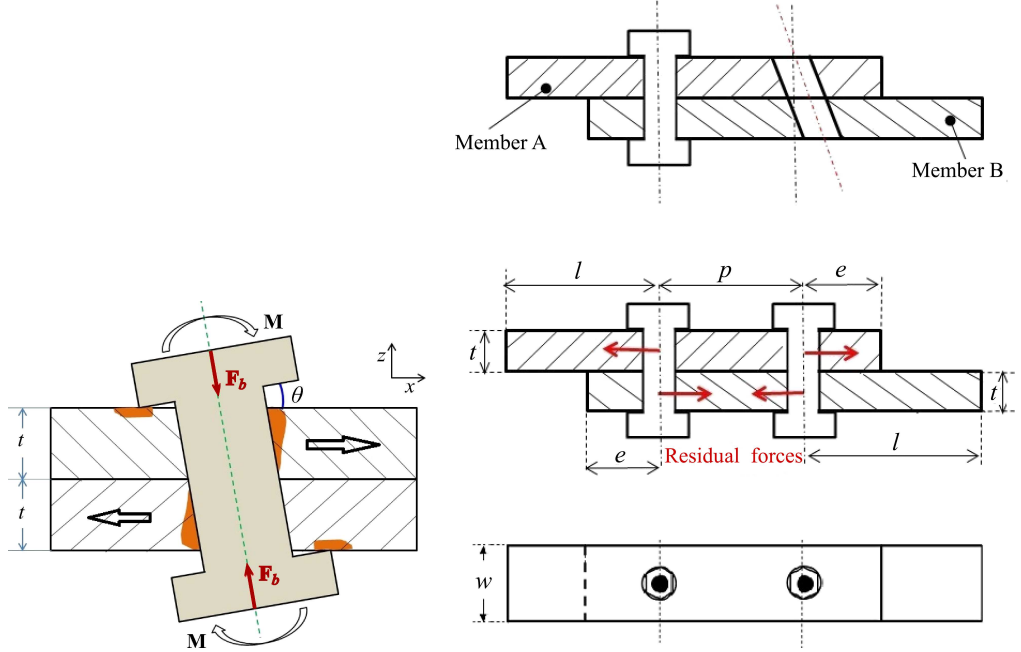


FIG. 1. Residual forces caused by hole perpendicularity error.

## 2. FINITE ELEMENT MODEL

This work focuses on single-lap double-bolt composite joints as illustrated in Fig. 1. The assembly, with a width  $w$ , is made of two composite plates with thickness  $t$ . Both of them, named Member A and B respectively, are fabricated using a carbon fiber/epoxy composite material and have a quasi-isotropic lay-up with stacking sequence [45/0/ - 45/90]<sub>5s</sub>. Each ply has a nominal thickness of 0.13 mm and 5.2 mm all together. Protruding head bolts are adopted and the geometrical parameters of the joints are listed in Table 1, where  $\phi_1$  and  $\phi_2$  indicate the diameters of shank and protruding head of the bolt, respectively.

**Table 1.** Geometrical parameters of composite joints [mm].

$t$	$l$	$p$	$e$	$w$	$\phi_1$	$\phi_2$
5.2	40	36	24	48	8	15

The material was modelled using homogeneous material properties and the elastic parameters are shown in Table 2. Note that  $E_{yy} = E_{xx}$ ,  $G_{yz} = G_{xz}$  and  $\nu_{yz} = \nu_{xz}$  are not listed in the table. The bolts are made from titanium alloy and its properties are also given in the same table.

**Table 2.** Material properties [14].

Homogenised laminate	$E_{xx}$ [GPa] 54.25	$E_{zz}$ [GPa] 12.59	$G_{xy}$ [GPa] 20.72	$G_{xz}$ [GPa] 4.55	$\nu_{xy}$ 0.309	$\nu_{xz}$ 0.332
Titanium	$E_b$ [GPa] 110	$G_b$ [GPa] 44	$\nu$ 0.29			

With the above geometrical parameters, a finite element model was first created using eight-node brick elements with incompatible modes (Fig. 2), C3D8I in Abaqus. The bolt, the washer and the nut are considered to be one solid piece for the sake of simplicity as well as to avoid the convergence problem.

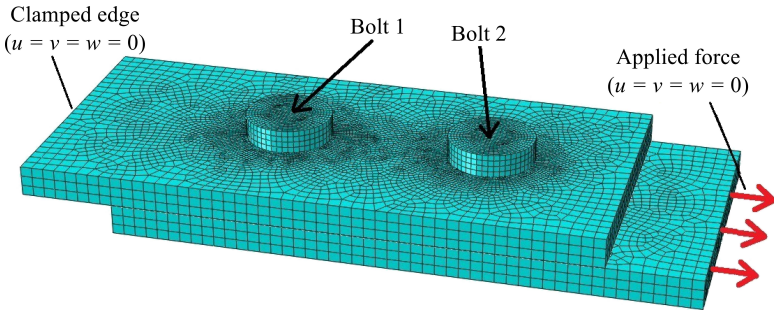


FIG. 2. The finite element model of the joint.

The contact between the surfaces in the joint is modeled using the general contact algorithm. All neighboring surfaces are considered to come into contact during the analysis including (i) contact between the laminates, (ii) contact between the bolts (shanks and heads) and the holes and (iii) contact between the nuts and the laminates. Finite sliding with a surface-to-surface option is applied for all possible contact, the penalty approach is used to enforce the contact constraints and Coulomb friction is assigned to all surfaces with a friction coefficient of 0.42 [6].

As shown in Fig. 2, the free end of Member A is clamped. To apply the force onto the free end of Member B, the motion of the surface was first constrained to a reference point chosen from the surface by using the coupling constraint available in Abaqus and a concentrated force was then applied to the reference point, which is not shown in Fig. 2.

Mesh refinement was performed to eliminate the influence of mesh size on computational accuracy. Considering the computation cost and accuracy, seeds with 2 mm wide edges are marked in black, 0.5 mm in red and 1 mm in green (Fig. 3). Since the detailed laminate stress analysis of the joint falls beyond the scope of this study, three elements are used across the thickness of the laminates.

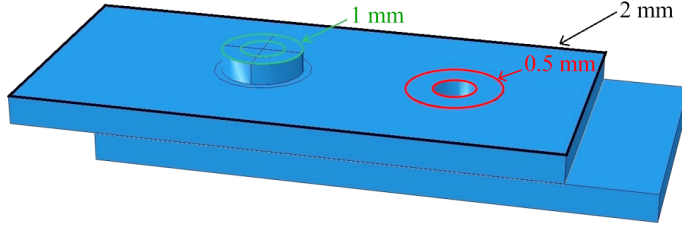


FIG. 3. Meshing strategy.

The total number of elements are almost 51k (Fig. 2) and it takes nearly 2.4 hours for one computation on a computer with i7 CPU and 32G memory.

### 2.1. Model validation

Mass-spring system has been widely used by many researchers to investigate the load distribution in multi-bolt composite joints [15–17]. The mass-spring system of single-lap double-bolt joints is shown in Fig. 4. The stiffness of the region designated “Member A” is signified by  $K_e$  and  $K_c$ , which indicate the spring stiffness between mass 1 and the free end, and the masses 1 and 3, respectively. A similar convention is used for Member B. The bolt stiffness is represented by  $K_b$ . The tensile load  $P$  is applied at mass 5. For the calculation of each stiffness, please refer to [15] for details.

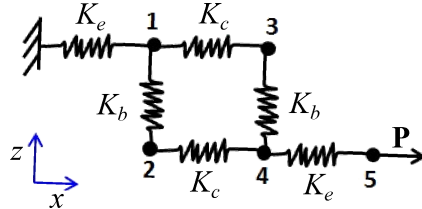


FIG. 4. Mass-spring system of single-lap double-bolt joints.

In the mass-spring system, the masses are free to move only in X direction and the springs have stiffness only in X direction too [15]. Based on these assumptions and under quasi-static loading, the stiffness equations for this system is given as

$$(2.1) \quad \begin{bmatrix} K_b + K_c + K_e & -K_b & -K_c & 0 & 0 \\ -K_b & K_b + K_c & 0 & -K_c & 0 \\ -K_c & 0 & K_b + K_c & -K_b & 0 \\ 0 & -K_c & -K_b & K_b + K_c + K_e & -K_e \\ 0 & 0 & 0 & -K_e & -K_e \end{bmatrix} \begin{bmatrix} x_1 \\ x_2 \\ x_3 \\ x_4 \\ x_5 \end{bmatrix} = \begin{bmatrix} 0 \\ 0 \\ 0 \\ 0 \\ P \end{bmatrix},$$

where  $x_i$  indicates the displacement of mass  $i$ .

Note that in this mass-spring system all factors including bolt torque, bolt-hole clearance and so forth are ignored. The load transfer ratio of bolts and assembly components can be easily computed using the following equations.

$$(2.2) \quad R_b = \frac{F_{b1}}{F_{b2}} = \frac{k_b(x_2 - x_1)}{k_b(x_4 - x_3)} = \frac{x_2 - x_1}{x_4 - x_3},$$

$$R_L = \frac{F_{L1}}{F_{L2}} = \frac{k_c(x_3 - x_1)}{k_c(x_4 - x_2)} = \frac{x_3 - x_1}{x_4 - x_2},$$

where  $R_b$  indicates the load transfer ratio of bolt 1 to bolt 2,  $F_{b1}$  and  $F_{b2}$  mean the loads transferred by bolt 1 and bolt 2 respectively,  $R_L$  signifies the load transfer ratio of Member A to Member B, and  $F_{L1}$  and  $F_{L2}$  are the loads transferred by Member A and Member B respectively.

Based on the above assumptions and under the condition that the two bolts are tightened with the same torque, it becomes easily known that  $R_b = 1.0$  and  $R_L = 1.0$  for the ideal single-lap double-bolt composite joints.

Given  $P = 10$  kN and two different bolt torques (0.5 Nm and 8 Nm), the displacements of all masses ( $x_i$ ,  $i = 1, \dots, 5$ ) obtained by numerical analysis are shown in Table 3. Note that both bolts share the same tightening torque in each computation. The bolt torque was simulated by normal compressive force  $F'_b$ , which is given by Eq. (2.3). As for the displacement for each mass, taking mass 3 as an example, the average displacement in  $X$  direction of all nodes on the small red circle in Fig. 3 is regarded as  $x_3$ . The load transfer ratios between bolts and laminates, as shown in the right two columns in Table 3, were calculated according to Eq. (2.2) with numerical outcomes. It can be seen that the results obtained by numerical simulation are in good agreement with theoretical ones as far as the load transfer ratio is concerned

$$(2.3) \quad F'_b = \frac{\tau}{k \cdot \phi_1},$$

where  $\tau$  is the bolt torque and  $k = 0.2$  is the torque coefficient [18, 19].

**Table 3.** Mass displacements and load transfer ratio.

Bolt torque [Nm]	$x_1$ [mm]	$x_2$ [mm]	$x_3$ [mm]	$x_4$ [mm]	$x_5$ [mm]	$R_b$	$R_L$
0.5	0.0279	0.1318	0.0370	0.1407	0.1680	1.0	1.0
8.0	0.0273	0.0999	0.0411	0.1137	0.1411	1.0	1.0

In addition, the accuracy of the proposed finite element model for predicting the load sharing behavior of single-lap double-bolt composite joints was verified by means of an experiment, too. As shown in Fig. 5, laminates are assembled

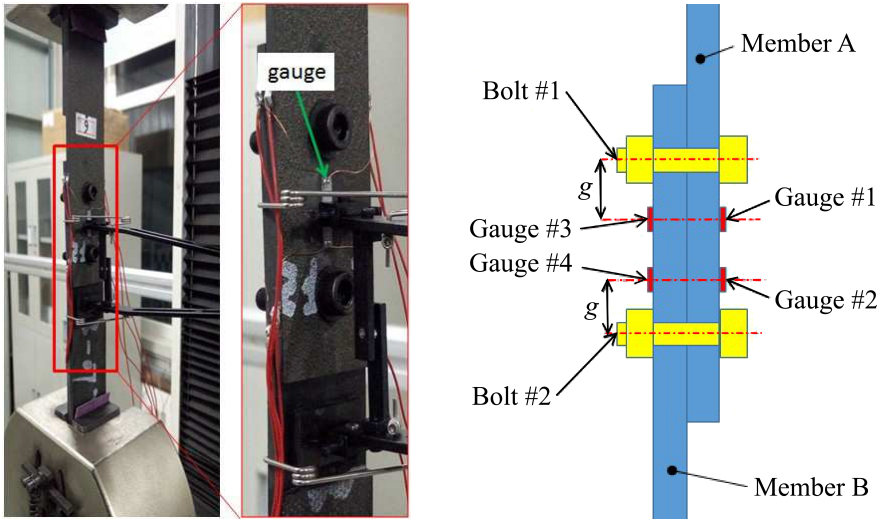


FIG. 5. Tensile experiment for single-lap double-bolt composite joints.

using two protruding bolts with the same bolt torque and a new drill is used to machine the two holes to avoid any possible damage and error. Four strain gauges are used to measure the strains of laminates and they are positioned symmetrically with respect to the distances from the gauges to the bolt holes. Considering the symmetry of the joint, the strains measured by gauges #1 and #4 should be consistent and the same should be the case for gauges #2 and #3. It must be noted here that the consistency of strains recorded by different gauges will be preserved as long as the assembly members, the two machined bolt holes and the applied bolt torques are the same. In other words, the material and manufacturing process used to produce the assembly members have no effect on the load distribution in the joint, although the recorded strains may vary according to the applied method.

The experiment was conducted on a universal test machine and a loading rate of 1 mm/min was adopted. The strains measured by the four gauges are shown in Fig. 6, where the horizontal axis represents load and the vertical one represents strain. The strains recorded by the four gauges at different loads are shown in Table 4, where  $\overline{R_L}$  indicates the average load transferred ratio by assembly members and  $\overline{R_L} = \frac{\#1+\#2}{\#3+\#4}$ . It can be seen that the loads transferred by the assembly members are almost equal, and with the increasing of load, the changes of strains at gauges #1 and #4, or #2 and #3 are similar to each other, which proves the reliability of the experiment and also shows the feasibility of using the numerical model to investigate the load distribution in single-lap multi-bolt composite joints.

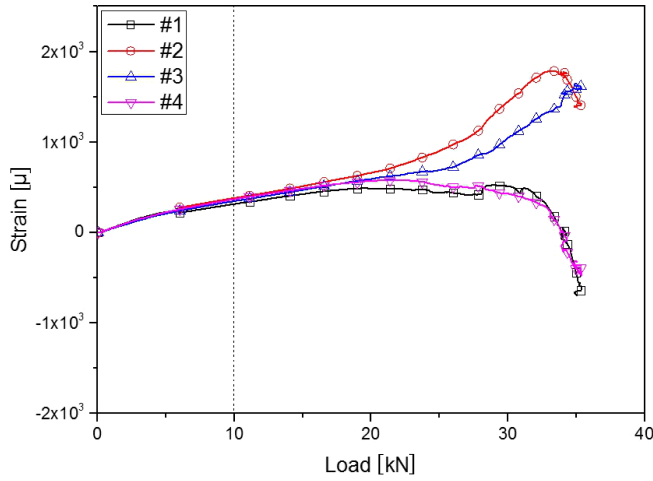


FIG. 6. Experimental strains of single-lap double-bolt composite joints.

**Table 4.** Strains obtained in experiment.

Load [kN]	#1 [ $\mu$ ]	#2 [ $\mu$ ]	#3 [ $\mu$ ]	#4 [ $\mu$ ]	$\bar{R}_L$
2	103	95	88	101	1.05
4	196	180	174	186	1.04
6	220	277	239	257	1.01
8	270	333	298	317	0.99
10	314	380	346	368	0.98

## 2.2. Parameters

As mentioned above, bolt hole may tilt along any direction in space when hole perpendicularity errors are involved. However, considering the potential influence of hole tilting direction on joint performance, two extreme cases are considered in this study as shown in Fig. 7. To differentiate between the two cases, the angle  $\alpha$  between the positive load orientation (blue arrows) and the positive hole direction (red arrows in Fig. 7) is used, where the orientation from

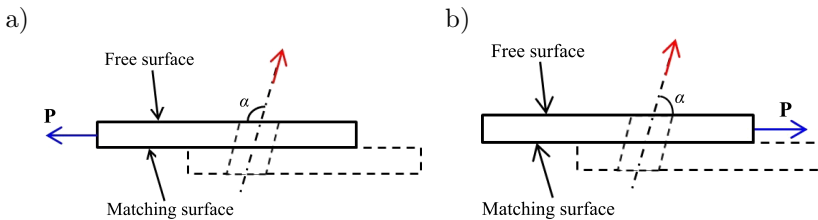


FIG. 7. Classification of hole tilting direction: a) against load direction, b) along load direction.

the matching surface to the free surface of an assembly member represents the positive hole direction. When  $\alpha < 90^\circ$ , the hole tilts along the load direction. Otherwise, it tilts against the load direction ( $\alpha > 90^\circ$ ).

After taking the symmetry of the joints into consideration, there are a total of five joint types for single-lap, double-bolt composite joints as shown in Fig. 8, where red solid lines indicate the real hole axes, black solid lines represent the composite laminates, dashed black lines signify the ideal axes of bolt holes and the black arrows are load orientations.

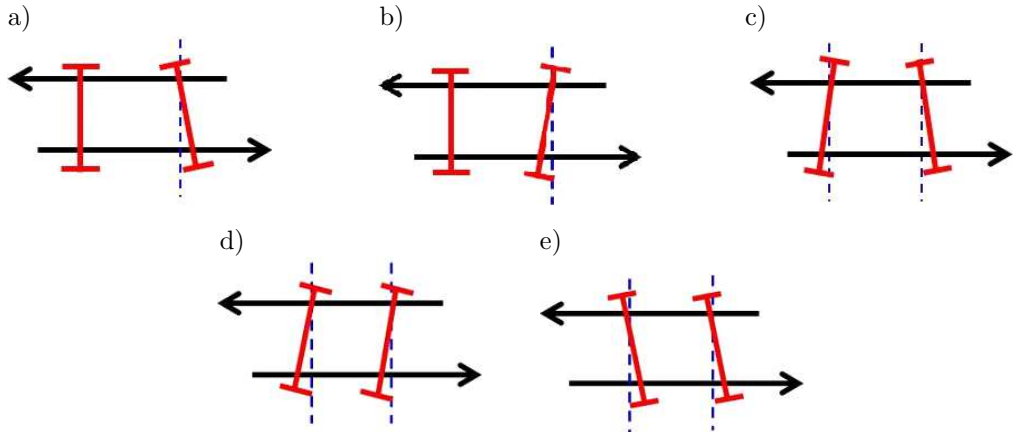


FIG. 8. The joint types of single-lap double-bolt composite joints with hole perpendicularity error considered: a) T1, b) T2, c) T3, d) T4, e) T5.

In addition, when the thickness of laminate  $t$  is given the magnitude of hole perpendicularity error can be represented by tilting angle  $\theta$  between the real axis of the bolt hole  $OC'$ , and ideal one  $OC$  in the cross-section defined by  $OC'$  and  $OC$  (Fig. 9). Note that this is based on the fact that, in practice, the hole is always drilled from one side of the assembly to the other. In addition, the

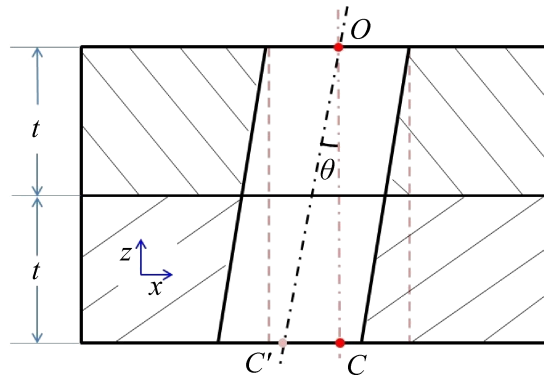


FIG. 9. Magnitude of perpendicularity error: tilting angle.

difference between  $\theta$  and  $\alpha$  lies in  $\alpha$  being defined with reference to the load direction. So, for the same hole the parameter  $\alpha$  may be different depending on the load direction. However, when a hole is machined, the parameter  $\theta$  is constant no matter how the load is transferred. Only with these two parameters, the directional characteristic of composite can be fully captured.

The parameters to be investigated are shown in Table 5, including the five joint types to reflect effects of hole tilting direction on joint performance, tilting angle  $\theta$  and two different bolt torques. The bolt torques were implemented using a bolt pre-tension section in 3D FE models and the normal compressive force  $F'_b$  produced by the bolt torque is obtained by Eq. (2.3).

**Table 5.** Parameters.

Type of joint	T1, T2, T3, T4, T5
Tilting angle $\theta$ [°]	1, 2, 3, 4
Bolt torque $\tau$ [Nm]	$\tau_1 = 0.5$ , $\tau_2 = 8$

### 3. RESULTS AND DISCUSSION

Parametric study was conducted to analyze the influences of tilting angle, bolt torque and joint type on the load distribution in single-lap, double-bolt composite joints and results are shown and discussed in this section.

#### 3.1. Influences on bolt transferred loads

The influences of joint type, bolt torque and tilting angle on bolt transferred loads are shown in Fig. 10, where the caption  $T_i - \tau_j - \tau_k$  means that the joint type is  $T_i$  and the bolt torques applied to bolt #1 and #2 are  $\tau_j$  and  $\tau_k$  respectively. It is that when the bolt torque is relatively low ( $\tau_1$ ), the joint type has hardly any effect on bolt-transferred load (Fig. 10a, 10c and 10e). The loads transferred by bolts show a good balance. However, with the increasing bolt torque the effect of joint type on load distribution in bolts becomes apparent. For the joint type  $T_1$ , the bolt in the hole without perpendicularity error takes more loads than the other and the proportion increases along with the increase of  $\theta$  (Fig. 10b). However, for  $T_2$ , the influences can be ignored even when  $\theta$  increases up to 4°. Comparing Fig. 10b to Fig. 10d, it can be found that when the hole tilts along the load direction the bolt in it will take on less loads. But when the hole tilts against the load direction, the bolt will take on more although the difference is not significant. As for  $T_3$ , the effect of increasing  $\theta$  on loads transferred by bolts can be ignored at all times. Therefore, it can be concluded that the loads transferred by bolts are affected only by hole tilting direction. When the hole

tilts against the load direction (Bolt #1 in  $T_3$ ), the bolt takes more loads. The only influence of titling angle, if any is to enhance the impact caused by hole tilting direction.

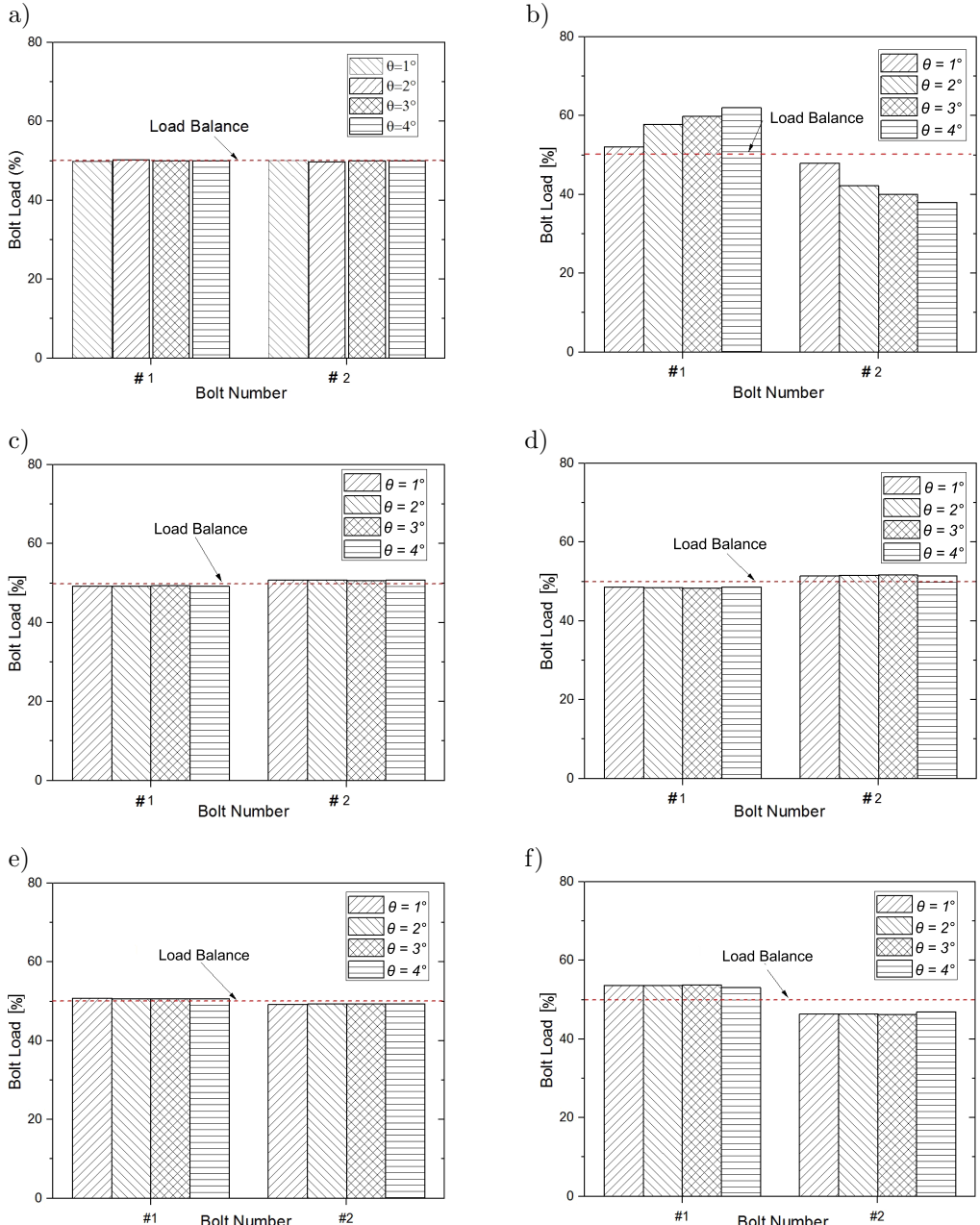


FIG. 10. The influences of  $T$ ,  $\tau$  and  $\theta$  on bolt transferred loads: a)  $T_1 - \tau_1 - \tau_1$ , b)  $T_1 - \tau_2 - \tau_2$ , c)  $T_2 - \tau_1 - \tau_1$ , d)  $T_2 - \tau_2 - \tau_2$ , e)  $T_3 - \tau_1 - \tau_1$ , f)  $T_3 - \tau_2 - \tau_2$ .

Taking  $T_3$  as an example, the effects of bolt torque on load distribution in bolts are shown in Fig. 11. When Fig. 11b is compared to Fig. 10e, it is found that the effect of bolt torque on bolt load distribution can be almost neglected. A similar conclusion can be drawn when Fig. 11a is compared to Fig. 10f. This means that when the hole tilts against the load direction, the bolt torque has little effect on bolt load distribution. But when Fig. 11a is compared to Fig. 10e or Fig. 11b to Fig. 10f, it can be seen that the differences between the loads transferred by the bolts become significant. This once again proves that when the hole tilts against the load direction, the increasing of bolt torque has little influence on bolt load distribution.

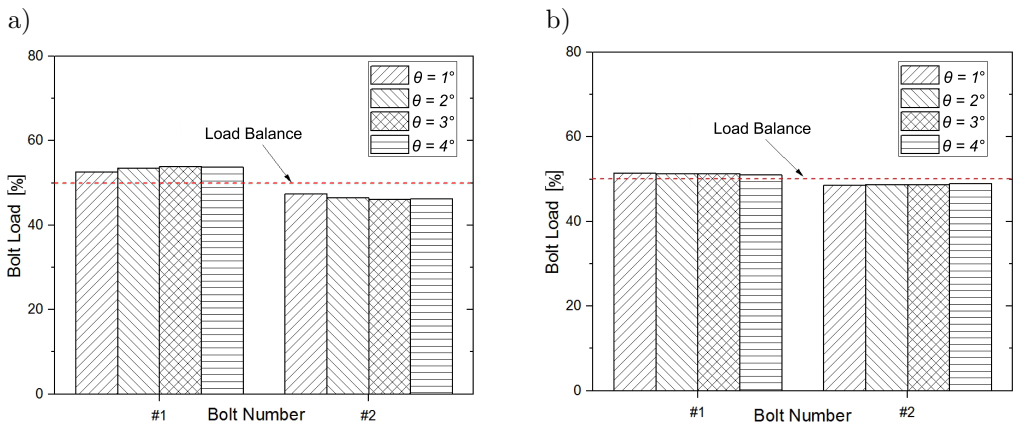


FIG. 11. The influences of bolt torque on bolt transferred loads: a)  $T_3 - \tau_1 - \tau_2$ , b)  $T_3 - \tau_2 - \tau_1$ .

As for  $T_4$  and  $T_5$ , the influences of bolt torque on bolt load distribution can be disregarded at all times.

### 3.2. Influences on laminate transferred loads

The influences of joint type, bolt torque and tilting angle on laminate transferred loads are shown in Fig. 12, where  $L1$  and  $L2$  indicate the top and bottom laminates, respectively, as illustrated in Fig. 8. It is found that for  $T_1$ , with the increasing of bolt torque the difference between the loads transferred by different laminates becomes apparent. Loads taken by the top laminate are almost twice as large as those of bottom one. For  $T_2$ , the increasing of bolt torque has hardly any effect on load distribution in laminates. The bottom laminate takes more than 60% of the tensile load. As for  $T_3$ , the increasing of bolt torque makes the top laminate take more loads. For all the cases, the increasing of  $\theta$  has no effect on load distribution in laminates.

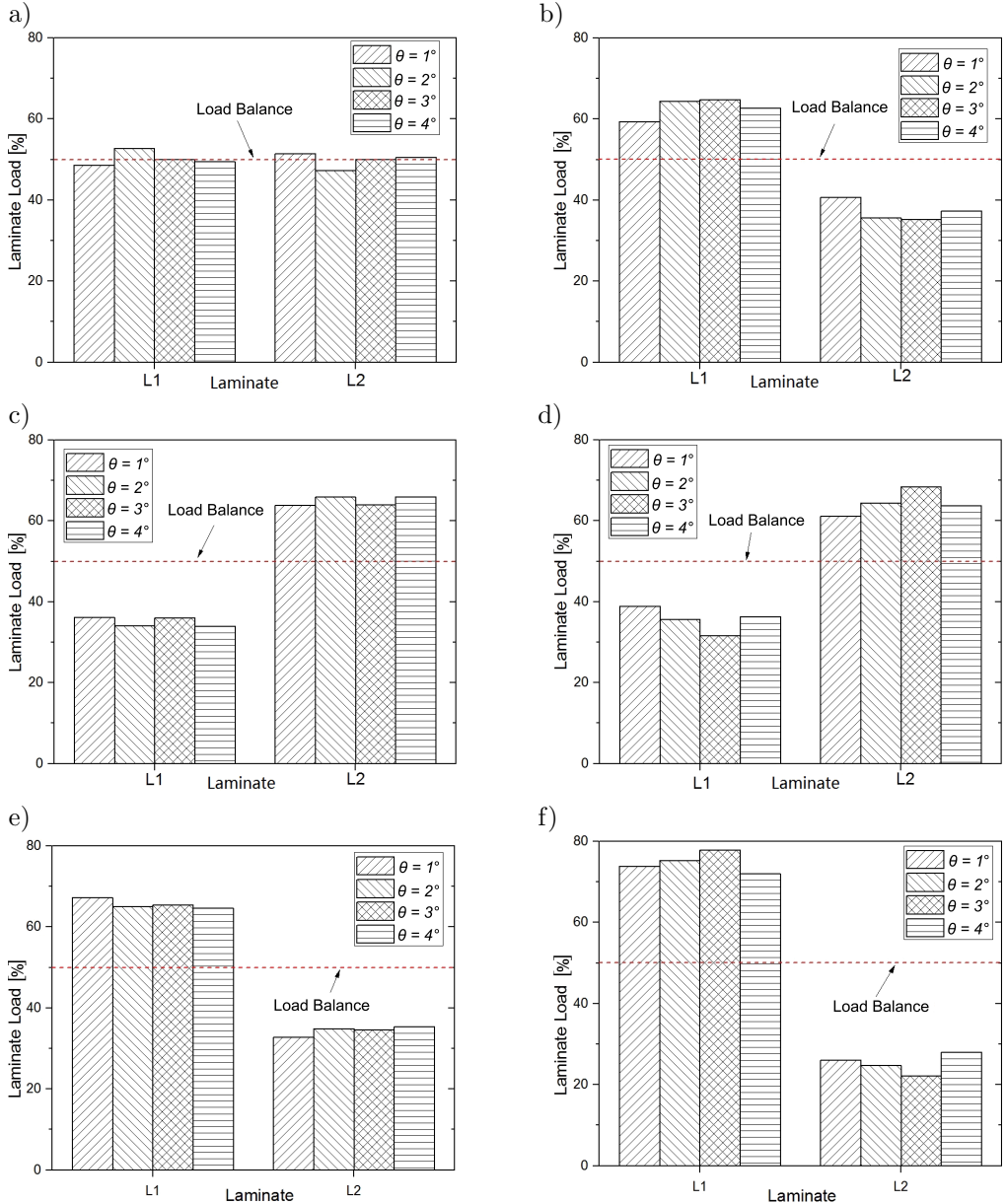


FIG. 12. The influences of  $T$ ,  $\tau$  and  $\theta$  on laminate transferred loads: a)  $T_1 - \tau_1 - \tau_1$ , b)  $T_1 - \tau_2 - \tau_2$ , c)  $T_2 - \tau_1 - \tau_1$ , d)  $T_2 - \tau_2 - \tau_2$ , e)  $T_3 - \tau_1 - \tau_1$ , f)  $T_3 - \tau_2 - \tau_2$ .

To verify the results obtained by numerical simulation, an experiment was conducted and the results are shown in Fig. 13. As shown in Fig. 13a, the joint type  $T_2$  is adopted and  $\theta = 4^\circ$  is selected. The strain gauges are located as

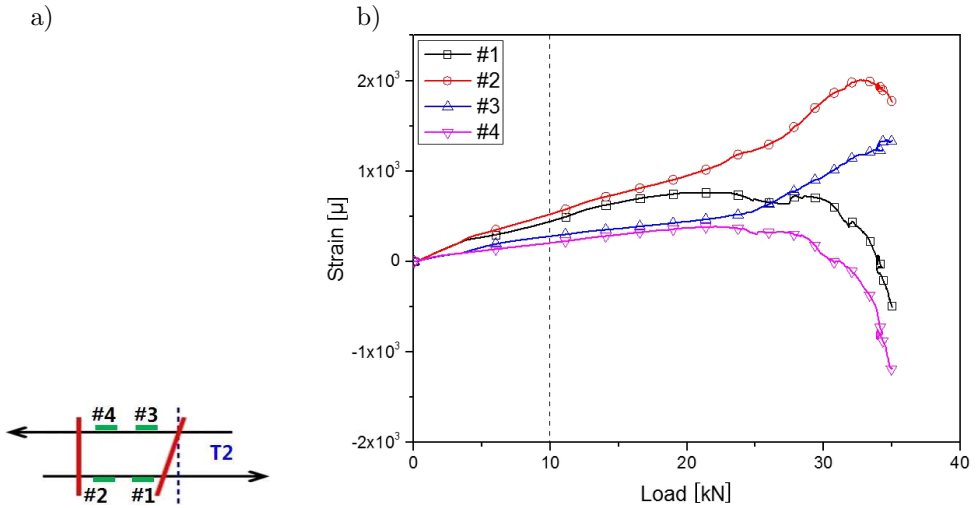


FIG. 13. Experimental results of load distribution in laminates.

shown in the figure. It can be seen from Fig. 13b that the trends in changing of the strains recorded by gauges #1 and #4 or by #2 and #3 are similar, which proves the accuracy of the experimental results.

The strains measured by gauges during experiment at different loading stages are shown in Table 6. It is observed that the bottom laminate takes almost twice as much load as the top one. According to the simulation result, the bottom laminate takes nearly 64% of the tensile load, which is 1.8 times of the load taken by the top one. It should be noted here that it is impossible to machine the two bolt holes as perfectly as expected, especially for the tilting angle. Differences must exist between them, which result in difference between the measured data. In either way the experimental results prove again the accuracy of this numerical study.

**Table 6.** Strains obtained in experiment.

Load [kN]	#1 [μ]	#2 [μ]	#3 [μ]	#4 [μ]	$\bar{R}_L$
2	126	122	63	67	1.85
4	243	262	114	101	2.35
6	297	350	194	137	1.99
8	368	440	245	173	1.97
10	442	522	279	205	2.02

The influences of bolt torque on load distribution in laminates are shown in Fig. 14. It is observed that the effect of increasing bolt torque is only to enhance

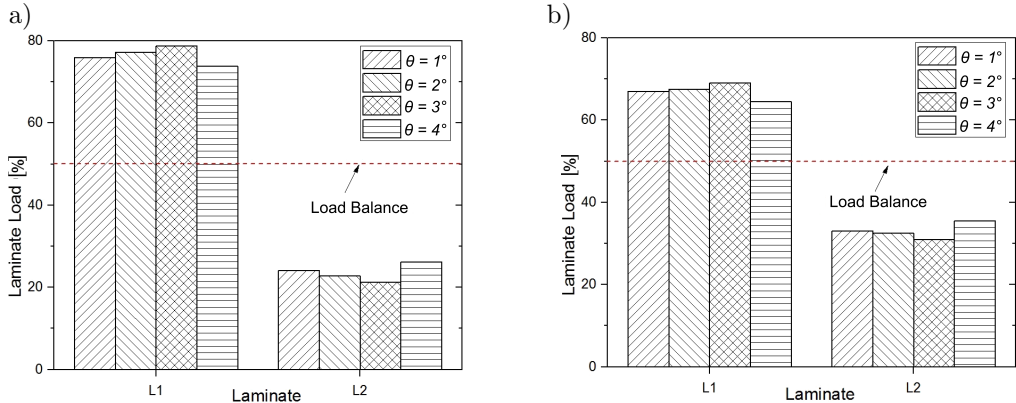


FIG. 14. The effects of bolt torque on load distribution in laminates: a)  $T_3 - \tau_1 - \tau_2$ , b)  $T_3 - \tau_2 - \tau_1$ .

the effect of hole tilting direction on the load distribution in laminates, which demonstrates good agreement with the conclusion drawn above.

#### 4. CONCLUSIONS

In this study, a finite element model was developed and used to investigate the influences of hole perpendicularity error and bolt torque on load distribution in single-lap double-bolt composite joints. Experimental results were used to verify the reliability of the numerical study. From the results shown in this paper, the following conclusions can be drawn:

- The hole tilting direction greatly influences load distribution in composite joints. When the hole tilts against the load direction, the bolt in it will take more loads. Otherwise, it will take less. As for the loads taken by assembly components, the hole tilting direction may induce a bad balance and make one of them take more than 60% of the load, which should be considered during design.
- The influence of tilting angle is very limited, and it can be ignored in many cases.
- The influence of bolt torque is to enhance the influences of hole tilting direction.

#### COMPETING INTERESTS

The authors declare that there is no conflict of interests regarding the publication of this paper.

## ACKNOWLEDGMENTS

This work was supported by the National Natural Science Foundation of China [No. 51375068,51475073], the Major State Basic Research Development Program [grant number 2014CB046504] and the Scientific Research Foundation for the Returned Overseas Chinese Scholars, State Education Ministry. The authors would like to acknowledge the above financial supports.

## REFERENCES

1. STANLEY W.F., McCARTHY M.A., LAWLOR V.P., *Measurement of load distribution in multi-bolt, composite joints, in the presence of varying clearance*, Journal of Plastics, Rubber and Composites, **31**(9): 412–418, 2002.
2. McCARTHY M.A., LAWLOR V.P., STANLEY W.F., McCARTHY C.T., *Bolt-hole clearance effects and strength criteria in single-bolt, single-lap, composite bolted joints*, Composites Science and Technology, **62**(10–11): 1415–1431, 2002.
3. SOYKOK I.F., *End geometry and pin-hole effects on axially loaded adhesively bonded composite joints*, Composites Part B: Engineering, **77**: 129–138, 2015.
4. XIE Z.H., LI X., GUO J.P., XIONG X., DANG X., *Load distribution homogenization method of multi-bolt composite joint with consideration of bolt-hole clearance*, Acta Materiae Compositae Sinica, **33**(4): 806–813, 2016.
5. LIU L., MAO Y., WEI R., *An analytical tool to predict load distribution of multi-bolt single-lap thick laminate joints*, [in:] Proceedings of the 18th International Conference on Composite Materials(ICCM), Jeju Island, Korea, pp. 1–8, 2011.
6. McCARTHY C.T., GRAY P.J., *An analytical model for the prediction of load distribution in highly torqued multi-bolt composite joints*, Composite Structures, **93**(2): 287–298, 2011.
7. ANDRIAMAMPIANINA J., ALKATAN F., STÉPHAN P., GUILLOT J., *Determining load distribution between the different rows of fasteners of a hybrid load transfer bolted joint assembly*, Aerospace Science and Technology, **23**(1): 312–320, 2012.
8. ZHOU Y., FEI Q., TAO J., *Profile design of loaded pins in composite single lap joints: from circular to non-circular*, Results in Physics, **6**: 471–480, 2016.
9. SHAROS P.A., EGAN B., McCARTHY C.T., *An analytical model for strength prediction in multi-bolt composite joints at various loading rates*, Composite Structures, **116**: 300–310, 2014.
10. LECOMTE J., BOIS C., WARGNIER H., WAHL J.-C., *An analytical model for the prediction of load distribution in multi-bolt composite joints including hole-location errors*, Composite Structures, **117**: 354–361, 2014.
11. TAHERI-BEHROOZ F., SHAMAEI KASHANI A.R., HEFZABAD R.N., *Effects of material nonlinearity on load distribution in multi-bolt composite joints*, Composite Structures, **125**: 195–201, 2015.
12. GÓMEZ S., OÑORO J., PECHARROMÁN J., *A simple mechanical model of a structural hybrid adhesive/riveted single lap joint*, International Journal of Adhesion & Adhesives, **27**(4): 263–267, 2007.

13. MORONI F., PIRONDI A., KLEINER F., *Experimental analysis and comparison of the strength of simple and hybrid structural joints*, International Journal of Adhesion & Adhesives, **30**(5): 367–379, 2010.
14. McCARTHY M.A., McCARTHY C.T., LAWLOR V.P., STANLEY W.F., *Three-dimensional finite element analysis of single-bolt, single-lap composite bolted joint. Part I – model development and validation*, Composite Structures, **71**: 140–158, 2005.
15. McCARTHY M.A., McCARTHY C.T., PADHI G.S., *A simple method for determining the effects of bolt-hole clearance on load distribution in single-column multi-bolt composite joints*, Composite Structures, **73**(1): 78–87, 2006.
16. OLMEDO A., SANTIUSTE C., BARBERO E., *An analytical model for predicting the stiffness and strength of pinned-joint composite laminates*, Composites Science and Technology, **90**: 67–73, 2014.
17. WANG P., HE R., CHEN H., ZHU X., ZHAO Q., FANG D., *A novel predictive model for mechanical behavior of single-lap GFRP composite bolted joint under static and dynamic loading*, Composites: Part B, **79**: 322–330, 2015.
18. PARK H., *Effects of stacking sequence and clamping force on the bearing strengths of mechanically fastened joints in composite laminates*, Composite Structures, **53**(2): 213–221, 2001.
19. QIN T., ZHAO L., ZHANG J., *Fastener effects on mechanical behaviours of double-lap composite joints*, Composite Structures, **100**: 413–423, 2013.

*Received May 3, 2017; accepted version September 30, 2017.*

---